Available online at www.sciencedirect.com
SCIENCE DIRECT®
Journal of Magnetic Resonance 174 (2005) 125–132
JMR Journal of Magnetic Resonance
www.elsevier.com/locate/jmr

^{13}C Direct detected experiments: Optimization for paramagnetic signals

Ivano Bertini *, Beatriz Jiménez, Mario Piccioli

Magnetic Resonance Center, University of Florence, Via L. Sacconi 6, 50019 Sesto Fiorentino, Florence, Italy

Received 19 October 2004; revised 12 January 2005

Abstract

To optimize ^{13}C direct detected experiments for the observation of signals close to a paramagnetic center, we have assessed the sensitivity of different sequences based on C^O–C^{ali} coherence transfer. Features of CACO experiments were tested for Calbindin D_{9k}, in which one of the two native Ca^{2+} ions is replaced by the paramagnetic Ce^{3+} ion. We have studied the comparison of single vs multiple quantum coherence transfer evolution as well as the influence of in-phase vs anti-phase detection of $^{13}C^O$ signals and finally the comparison of a coherence transfer step based on a C^O_y in plane with respect to a C^{ali}_y in plane. The acquisition of the anti-phase component of the signal, accomplished by the removal of the last refocusing steps, allowed the identification of some signals unobserved with other pathways. The structural dependency of paramagnetism-induced nuclear relaxation is such that the identification of the most suitable coherence transfer pathway is not known "a priori" but it is driven by the relative proximity of C^{ali} and C^O to the paramagnetic center.

Keywords: ^{13}C Direct detection; Paramagnetic NMR; Hyperfine interaction; (CO)CACO; CACO

1. Introduction

Formerly considered as an enclave for inorganic chemists and metalloprotein biochemists, NMR spectroscopy of paramagnetic systems is now a versatile tool for structural biologists [1,2]. Indeed, paramagnetic probes have been recently exploited for fashionable applications in NMR spectroscopy. For example, they have been used to map interaction sites using relaxation induced selective broadening [3–8], to obtain long-range constraints or to induce self-orientation in diamagnetic molecules [9–11], and to refine structure calculations [12–16]. Within this frame, we are interested in analyzing features and limitations of coherence transfer based on ^{13}C direct detection [17–20], which can be a unique source of structural information in the proximity of a paramagnet [21,22]. Hyperfine contributions to relaxation have a γ^2 dependency which fostered low gamma nuclei NMR studies [23–28]. Pioneering studies [29–33] were carried out well before a new generation of high sensitivity probes became available [20,34,35].

We focused on the protein Calbindin D_{9k} [36,37] in which the native Ca^{2+} in site II has been replaced by Ce^{3+} [13,37,38]. This molecule has been widely used as test system to assess novel NMR methodologies in paramagnetic molecules [14,15,22,39,40]. Because calcium binding sites are constituted by carboxylate or carbonyl ligands [41], ^{13}C direct detection has already been shown to be a very efficient approach to characterize the first coordination sphere [21]. The metal center at site II is shown in Fig. 1. Ce^{3+} is coordinated by the carboxyl groups of two aspartate residues (Asp 54 and 58), and by a bidentate glutamate ligand (Glu 65). The coordination sphere is completed with two carbonyls of amide groups, one from Asn 56 side chain and the other from Glu 60 backbone.

* Corresponding author. Fax: +39 55 4574 271.
E-mail address: bertini@cerm.unifi.it (I. Bertini).

1090-7807/$ - see front matter © 2005 Elsevier Inc. All rights reserved.
doi:10.1016/j.jmr.2005.01.014

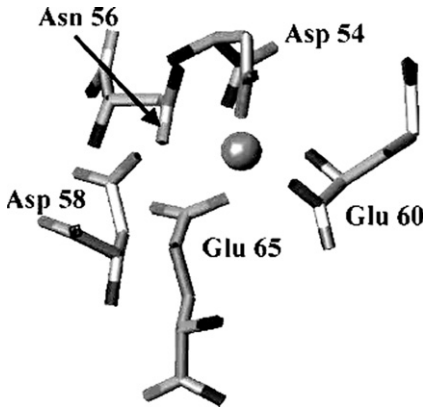

Fig. 1. The metal site II in Calbindin D_{9k}. Residues bound to Ce^{3+} are shown.

The efficiency of coherence transfer between two ^{13}C nuclei within the first coordination sphere is expected to be substantially quenched by paramagnetism-induced relaxation, which under these conditions is the dominant contribution to nuclear relaxation [22]. Therefore the intensity of C^{O}–C^{ali} connectivities of the metal coordinating groups can be used as a marker to monitor the efficiency of different experimental schemes. Because C^{O} detection seems to be the most promising approach to exploit ^{13}C direct detection to obtain sequence specific assignment [42], we focused our study on the C^{ali}–C^{O} transfer (both backbone C^{α}–C^{O} and side chain C^{β}–C^{γ}, C^{γ}–C^{δ}) with C^{O} detection. The analysis of various coherence transfer pathways will constitute the background to design and implement protonless pulse sequences, which have been recently proposed to be an important avenue to open new perspectives in biomolecular NMR. We basically considered three variables: (I) the use of a single quantum (SQ) vs multiple quantum[1] (MQ) coherence transfer, (II) the acquisition of an anti-phase doublet vs an in-phase doublet, and (III) a coherence transfer step based on an in plane C^{O}_{y} with respect to an in plane C^{ali}_{y}.

2. Experimental

2.1. Sample preparation

Protein expression [43] and purification [44] of the bovine Pro43-Met43 mutant of Calbindin D_{9k} was performed as previously reported [45,46] in M9 minimal medium containing $(^{15}NH_4)SO_4$ and [$^{13}C_6$]glucose as the sole sources of nitrogen and carbon, respectively. The replacement of Ca^{2+} with Ce^{3+} at site II was performed as already described [38]. Samples for NMR experiments were about 600 μl volume, 1 mM concentration at pH 6.0, in unbuffered water solutions.

2.2. NMR spectroscopy

All the experiments presented in this work have been tailored for the acquisition of fast relaxing signals. The spectra were recorded at 300 K on a Bruker Avance 700 (16.4 T) equipped with a triple resonance probe, with *z*-axis gradients, which inner coil has been tuned and optimized to ^{13}C direct detection (TXO probe, hereafter). Carbon Larmor Frequency was 176.1 MHz.

All CACO experiments were collected using the same set of acquisition parameters. We used Q5 Gaussian cascade [47] of 333 μs length for 90° pulses, and Q3 Gaussians cascades of 220 μs for 180° pulses. Each pulse was defined by 1000 points. They provide a bandwidth excitation over 20980 Hz (119.18 ppm) and 25740 Hz (146.22 ppm) respectively. A 50 μs rectangular pulse was used for C^{O} refocusing during C^{ali} evolution period. All pulses were applied at frequencies of 189 and 40 ppm for C^{O} and C^{ali}, respectively. Spectral windows of 200 and 80 ppm were used for the C^{O} and C^{ali} dimensions. $^{13}C^{O}$, $^{13}C^{ali}$, ^{15}N, and ^{1}H carriers were set at 108, 40, 120, and 3.5 ppm, respectively. For each experiment 2048×128 real data points matrices were acquired using t_{1max} (C^{ali}) and t_{2max} (C^{O}) of 8.9 and 29.1 ms, respectively. The coherence transfer for $^{13}C^{O}$–$^{13}C^{ali}$ coupling (typically $1/2J = 9.1$ ms) was shortened to 5.5 ms to avoid the loss of paramagnetic signals by relaxation. TPPI [48] was used to obtain quadrature detection in the indirect dimension. Typically 512 scans each fid were collected, using a recycle delay of 300 ms. The total length of each experiment was 6 h and 40 min. ^{15}N and ^{1}H were decoupled using garp4 [49] and waltz16 [50] schemes, respectively. All experiments were processed with the Bruker XWINNMR software package.

3. Results

In paramagnetic systems, paramagnetism-induced relaxation quenches signal intensities during coherence transfer and chemical shift evolutions steps [22,51]. In homonuclear cases, provided that cross correlation effects are not playing a major role [52,53], COSY is the best approach to detect scalar couplings involving broad resonances, because relaxation is active only during t_1 and t_2. An appropriate choice of t_{1max} and t_{2max} during processing may reach the best compromise between coherence transfer evolution and relaxation losses [54,55]. Fig. 2 shows the results of a magnitude COSY in which signals belonging to residues directly coordinated to the metal center are pointed out, as well as some other signals arising from the immediate proximity

[1] *Abbreviations used:* MQ, multiple quantum; SQ, single quantum; IP, in-phase; AP, anti-phase; C^{ali}, aliphatic carbon; C^{O}, carbonyl; TPPI, time proportional phase incrementation.

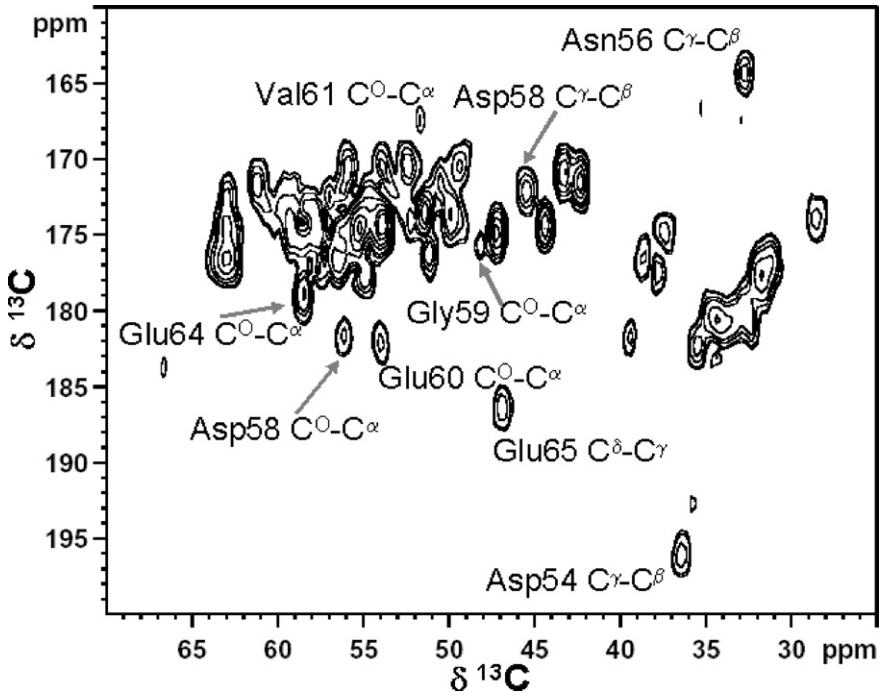

Fig. 2. ^{13}C–^{13}C COSY experiment, on CaCeCb, collected at 176 MHz, 300 K. Only the spectral region involving connectivities between quaternary carbon resonances (F_1) and carbon resonances of aliphatic carbons (F_2) is shown. Assignment of signals close to the paramagnetic center are reported.

of the paramagnetic center. They have been previously assigned [21] via an analogous ^{13}C COSY experiment collected on a conventional probe with an inner broadband coil (BBO). The use of a customized probe for triple resonance, with inner ^{13}C coil for direct detection reduces the experimental time for a COSY experiment tailored to paramagnetic systems to about 6 h.

INEPT-like or multiple quantum coherence experiments would be the obvious alternative approach with respect to a simple COSY experiment. Their advantage is that coherence transfer is selectively directed vs a specific transfer pathway. The insertion of a constant delay for coherence transfer optimizes the transfer function but also contributes to relaxation. In longer pulse sequences the loss of signal intensity due to relaxation plays a critical role. Therefore, optimization of the basic building blocks is mandatory for successful implementation of the sophisticated pulse sequences used in structural biology [56].

The pulse sequences we developed are reported in Fig. 3. Sequences A and B correspond to "classical" multiple quantum and single quantum coherence transfer steps, according to the out and back scheme of conventional HMQC [57] and HSQC [58] experiments. To rationalize the various possible pathways for coherence transfer, we will name the sequences accordingly [59]. Sequence A is therefore called (CO)CACO-MQ and sequence B is (CO)CACO-SQ. Magnetization is transferred out and back from the C^O spins, C^{ali} is evolved in the indirect dimension while ^{15}N and ^{1}H are decoupled throughout the entire sequence. (CO)CACO-MQ sequence has been already used with and without homodecoupling of C^{ali} spins during $^{13}C^O$ acquisition [25,26]. In the case of fast relaxing signals, homonuclear decoupling accomplished via adiabatic broad band decoupling [60,61] resulted in up to 50% signal loss. More recently, the IPAP approach [62,63] has been proposed to remove strong C^O–C^{ali} coupling during C^O acquisition [64]. When dealing with diamagnetic signals, this scheme is far more efficient than adiabatic decoupling and provides much better quality spectra. Still, IPAP cannot be used for detection of fast relaxing signals, because of the additional refocusing period required for the IPAP scheme.

Sequences 3C and 3D correspond to (CO)CACO-MQ and (CO)CACO-SQ but without the refocusing period at the end of t_1 evolution. Signals are therefore acquired as anti-phase doublets. The (CO)CACO-MQ-AP sequence has some additional modifications with respect to (CO)CACO-MQ. Two 180° pulses are required to refocus chemical shift evolution during the outward transfer [57]. A z-filter with a crush gradient is also added at the end of the sequence, to remove possible artifacts. The (CO)CACO-SQ-AP corresponds directly to the CRINEPT sequence [65] with an additional 180° pulse on the C^{ali} to avoid Bloch–Siegert effects [66]. Finally, sequence 3E is a single quantum experiment which is based on a $C^{ali} \rightarrow C^O$ coherence transfer step. At variance with sequence D, carbonyl spins are maintained along the z axis during the build-up of trans-

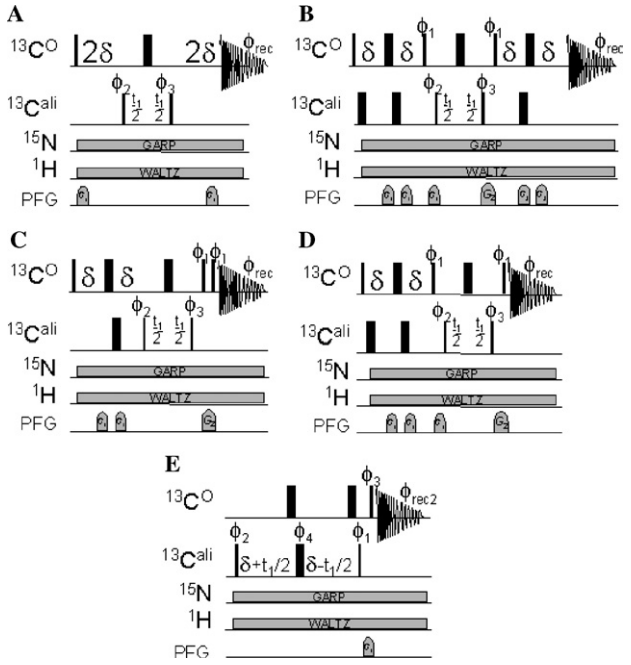

Fig. 3. Different sequences for CACO experiments: (A) (CO)CACO-MQ; (B) (CO)CACO-SQ; (C) (CO)CACO-MQ-AP; (D) (CO)CACO-SQ-AP; and (E) CACO-SQ-AP. Narrow and wide bars represent 90° and 180° pulses. All pulses are selective but the 180° C^O during C^{ali} evolution. 90° pulses are Q5 Gaussian cascade, 180° pulses are Q3 Gaussian cascade, defined as in the experimental part. Delay δ has been set at 2.7 ms to optimize detection of paramagnetic signals. Phase cycle is x unless otherwise indicated, and $\phi_1 = y$; $\phi_2 = x, -x$; $\phi_3 = x, x, -x, -x$; $\phi_4 = x, x, x, x, y, y, y, y$; $\phi_{rec} = x, -x, -x, x$; $\phi_{rec2} = x, -x, -x, x, -x, x, x, -x$. Pulse field gradients are sine shaped with duration of 1 ms and strength $G1_z = 7$ G/cm, $G2_z = 12$ G/cm, $G3_z = 10.5$ G/cm.

fer function. Scalar coupling evolves via the $C^{ali}_y \rightarrow C^{ali}_x C^O_z$ rather than using the path $C^O_y \rightarrow C^O_x C^{ali}_z$ and acquisition is concatenated to J-coupling evolution in a constant time fashion. Like the (CO)CACO sequences, different acquisition schemes are possible in CACO. We can acquire the anti-phase doublet immediately after the two 90° mixing pulses, or after an IPAP block. Data from the previous experiments outline that anti-phase acquisition is by far more efficient in paramagnetic systems, we therefore discuss here only the CACO-SQ-AP sequence, reported in Fig. 3E.

We focus our attention on those signals, already identified, which arise from the first coordination sphere. In particular, we select signals arising from the Asp 54 and Asp 58 C^γ–C^β coherence transfer, as well as C^O–C^α arising from Gly 59. They are all observable in the COSY experiment reported in Fig. 2. Both Asp 54 and Asp 58 C^γ belongs to carboxyl groups which are covalently bound to Ce^{3+}. They experience hyperfine shifts of about +20 ppm for Asp 54 C^γ and −10 ppm for Asp 58 C^γ. Relaxation rates are 4.3 and 1.4 s^{-1} for R_1 and 120 and 70 s^{-1} for R_2, respectively. Gly 59 backbone connectivity has been selected as a sample case of backbone C^α–C^O which is close to the paramagnetic center although not directly bound to metal (5.7 and 5.3 Å away for C^α and C^O, respectively).

Fig. 4 shows the rows of the various CACO spectra for the three peaks mentioned above. Comparison of intensities among (CO)CACO and (CO)CACO-AP, for both MQ and SQ experiments, provides an estimate of the dramatic relaxation effects which take place during refocusing. The price to pay for the obtainment of in-phase signals (Figs. 4A and B) is the loss of, on average, 40–50% of observable magnetization for all residues in the first coordination sphere. In the case of CaCeCb, these effects are observed within a 9 Å sphere from the metal. Indeed, for the C^α–C^O connectivity of Glu 64, which are at 8.9 and 8.3 Å from Ce^{3+}, about 10% decrease in intensity is observed when passing from the anti-phase to the in-phase acquisition (data not shown). This demonstrates that detection of the anti-phase doublet is preferable to detection of the in-phase component, when the aim is to collect fast relaxing signals. The limited signal resolution and the paramagnetic induced broadening is such that, when signals are acquired as in-phase doublets, this can be completely unresolved, as in the case of Asp 54 C^γ and Gly 59 C^O in Figs. 4A and B. For anti-phase acquisition, partial cancellation between the two cross peak components may occur wherever paramagnetism-induced line broadening is larger than J-coupling splitting [55]. The values of C^O–C^α coupling constant and the γ^2 dependency of paramagnetic relaxation are such that mutual cancellation of anti-phase components is less crucial than in ^{1}H COSY spectra [54,55]. However, like the homonuclear ^{1}H case, a dispersion mode phase correction provides the maximum of signal intensity [54]. Fig. 4F reports the same 1D rows shown in Fig. 4E with an additional 90° zero order phase correction. For Asp 54 C^γ, which is a well isolated signal of a metal bound carboxylate, an about 20% increase in signal intensity is observed when the spectrum is phased in the dispersion mode. Such gain is not observed for signals far from the paramagnetic center or being in a more crowded region of the spectrum.

The same considerations are likely to hold in diamagnetic systems of large molecular mass. Indeed, fast transverse relaxation induced by slow molecular tumbling may provide a substantial loss of signal intensity and would eventually cause the loss of observable signals. The acquisition of in-phase doublets provide a spectrum easier to process than anti-phase doublets (either in absorption or in dispersion mode), especially in the frame of quantitative analysis of peak intensities [67,68]. Unfortunately, the refocusing delay of the MQ or SQ backward transfer can be sufficient to quench signal intensities.

Very similar intensities are observed when comparing SQ vs MQ experiments, in both refocused and non refocused versions. On average, slightly lower signals are ob-

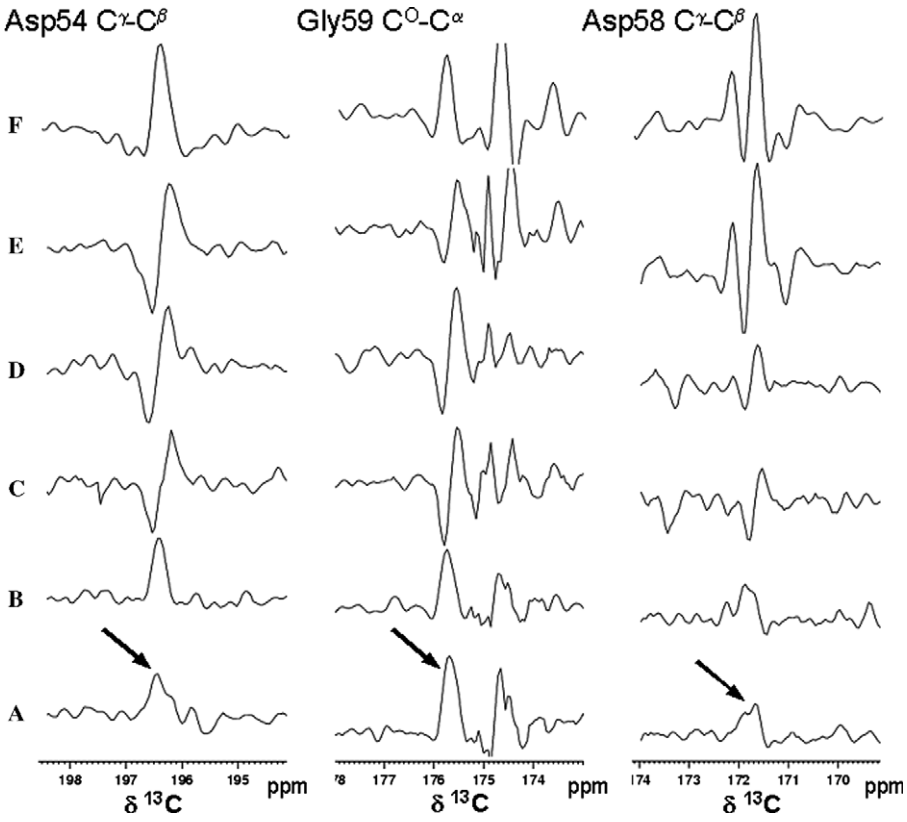

Fig. 4. Selected rows for three paramagnetic signals: Asp 54 C^{γ}–C^{β}, Gly59 C^{O}–C^{α}, and Asp 58 C^{γ}–C^{β}. Rows are extracted from experiments collected using the sequences described in Fig. 3: (A) (CO)CACO-MQ; (B) (CO)CACO-SQ; (C) (CO)CACO-MQ-AP; (D) (CO)CACO-SQ-AP; (E) CACO-SQ-AP; and (F) same as (E) but plotted with a 90° zero order phase shift. In all experiments digital resolution during acquisition is 34 Hz/Pt.

served in SQ pathways when comparing the in-phase sequences, i.e. (CO)CACO-MQ and (CO)CACO-SQ. The trend observed for Asp 54 in Fig. 4, which has a larger intensity in the (CO)CACO-SQ, is an exception with respect to the behavior of most of the signals affected by the paramagnetic center. The slightly higher sensitivity of (CO)CACO-MQ vs (CO)CACO-SQ is most likely due to some loss of magnetization that occurs during the INEPT step because the additional 180° pulses (two on C^{ali} and one on C^{O}) which are not present during the MQ step. Indeed, the two (CO)CACO-AP sequences, which basically have the same number of pulses, provide the same results also from a quantitative point of view (Figs. 4C and D). It is however clear that the type of coherence transfer is not the critical step of these sequences. To identify fast relaxing signals t_{1max} evolution must be kept very short. Under the above conditions, i.e., t_{1max} lower than 10 ms, the different relaxation features of SQ vs MQ will not substantially affect signal intensity, even for those signals which are at the limit of detectability.

The scenario is different when CACO-SQ-AP experiment is observed compared to the (CO)CACO-SQ-AP. At high field, even in the case of a small protein like Calbindin D_{9k}, Chemical Shift Anisotropy (hereafter CSA) will make $R_2^{C^O}$ larger than $R_2^{C^{ali}}$ [69]. Therefore, C^{O} CSA may have severe consequences in affecting sensitivity of most of the experiments which rely on C^{O} in plane coherence transfer. In the CACO-SQ-AP experiment, the relaxation of C^{ali}–C^{O} coherence transfer is dominated by the transverse relaxation of C_y^{ali}. Therefore signal losses due to relaxation are much lower than the complementary case of (CO)CACO-SQ-AP, in which relaxation is dominated by the stronger C_y^{O} transverse relaxation. In CACO-SQ-AP, the C^{O} magnetization is always on the z axis prior to the t_2 evolution. This provides, in the case of diamagnetic peaks, up to a 70% increase in signal intensity for backbone resonances and about a factor of 4 for side chain peaks, when compared to (CO)CACO-SQ-AP. The most significant evidence of the higher sensitivity of CACO-SQ-AP, is the observation of the two peaks arising from backbone Glu 60 and from side chain of Glu 65, which are both bound to Ce^{3+}. These peaks are below the threshold of detectability in (CO)CACO-SQ-AP (Fig. 5B) and could be quantitatively analyzed in the case of CACO-SQ-AP (Fig. 5C).

However, in the case of paramagnetic peaks, the higher sensitivity of CACO-SQ-AP is not a fixed rule, but it is structure dependent. This is indeed the case of Asp 54 side chain, for which the observed intensity in the CACO-SQ-AP experiment is the same as in the (CO)CACO-SQ-AP

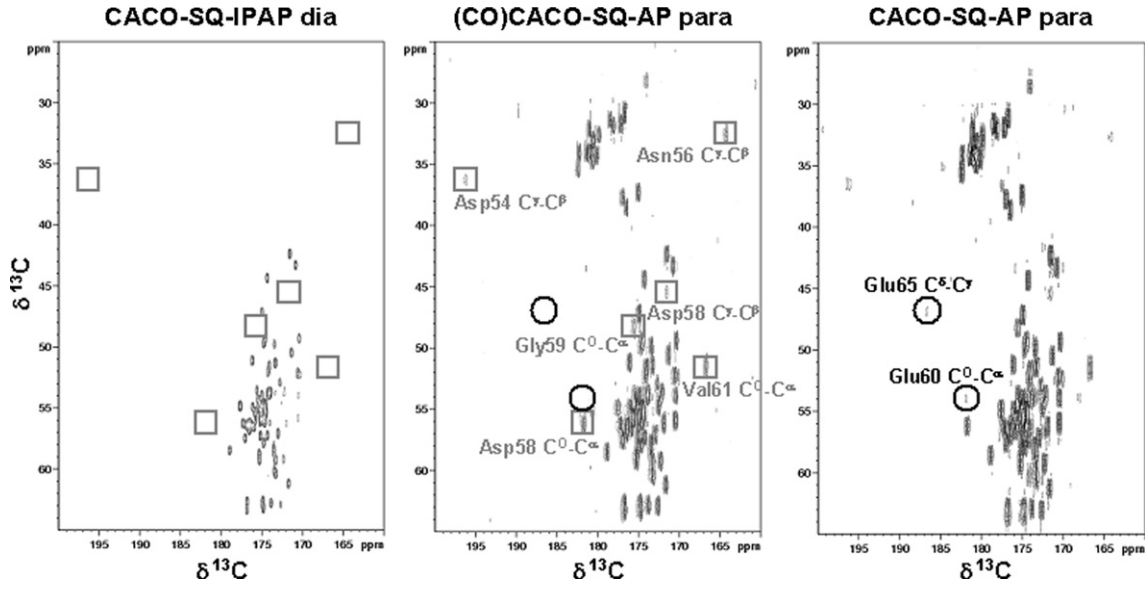

Fig. 5. CACO experiments collected on CaCeCb at 300 K, at 176 MHz. CACO-SQ-IPAP sequence optimized for diamagnetic signals ($\delta = 4.5$ ms, ns = 8, 256 points in f_2); (CO)CACO-SQ-AP and CACO-SQ-AP sequences tailored for paramagnetic signals. Squares show the paramagnetic signals which are not detected in the diamagnetic experiment, circles show the signals detected only with the CACO-SQ-AP sequence. All experiments are phased in absorption mode.

and in the case of Gly 59 for which, at variance with the general trend, signal intensity is weaker than that collected with (CO)CACO-SQ-AP (Fig. 4). The rationale of this behavior arises from the structural dependency of hyperfine relaxation. Hyperfine relaxation is dependent on r^{-6}, so for nuclei close to the paramagnetic center, this is the dominant contribution to relaxation. Thus, which of $C_y^O C_z^{ali}$ or $C_y^{ali} C_z^O$ relaxes faster, is not known "a priori," but will depend on the relative distances of C^O and C^{ali} from the paramagnetic center.

Overall, Fig. 5 summarizes the differences when passing from a "diamagnetic" CACO-IPAP experiment to a tailored (CO)CACO-SQ-AP and then to a CACO-SQ-AP. At the expense of signal resolution, the removal of IPAP and the removal of the refocusing of the anti-phase doublet leads to improve detection of fast relaxing signals as observed from the appearance in the 2D maps of six signals previously unobservable (Fig. 5B). Furthermore, the CACO-SQ-AP provides two additional signals that could not be detected with the (CO)CACO-SQ-AP sequence (Fig. 5C).

4. Conclusions

The use of ^{13}C direct detection in paramagnetic systems is a very promising technique to reduce the "blindness sphere" around a metal ion. While SQ and MQ coherence transfer in CACO type experiments do not show substantial differences in signal intensities close to the metal center, a sensitivity improvement is provided by the removal of the last refocusing step [65]. At variance with diamagnetic cases, ^{13}C relaxation of different spins is structure dependent and is therefore not predictable "a priori."

The assessment of the various possible pathways for a CACO transfer will be important to develop experimental protocols for the identification of signals close to the paramagnetic center. Furthermore, the optimization of such a coherence transfer is crucial for the obtainment of structural constraints arising from relaxation and cross correlation rates. The latter could be analyzed only when experiments are optimized to the detection of fast relaxing signals.

Acknowledgments

B.J. is a long term fellow of EMBO. B.J. thanks EU RTN "Cross correlation between the fluctuations of different interactions: a new avenue for biomolecular NMR" (Contract No. HPRN-CT-2000-00092) for a fellowship. This work was supported by COFIN-2003 (Nov 03–Nov 05) and by MIUR—FIRB, RBAU013 NSB, Italy.

References

[1] I. Bertini, C. Luchinat, M. Piccioli, Paramagnetic probes in metalloproteins. Turning limitations into advantages, Methods Enzymol. 339 (2001) 314–340.
[2] M. Ubbink, J.A.R. Worrall, G.W. Canters, E.J.J. Groenen, M. Huber, Paramagnetic resonance of biological metal centers, Annu. Rev. Biophys. Biomol. Struct. 31 (2002) 393–422.
[3] A.F. Frederick, L.E. Kay, J.H. Prestegard, Localization of divalent ion sites in acyl carrier protein using relaxation perturbed 2D NMR, FEBS Lett. 238 (1988) 43–48.

[4] A.M. Petros, L. Mueller, K.D. Kopple, NMR identification of protein surfaces using paramagnetic probes, Biochemistry 29 (1990) 10041–10048.
[5] M. Scarselli, A. Bernini, C. Segoni, H. Molinari, G. Esposito, A.M. Lesk, F. Laschi, P. Temussi, N. Niccolai, Tendamistad surface accessibility to the TEMPOL paramagnetic probe, J. Biomol. NMR 15 (1999) 125–133.
[6] S. Vathyam, R.A. Byrd, A.F. Miller, Mapping the effects of metal ion reduction and substrate analog binding to Fe-superoxide dismutase by NMR spectroscopy, Magn. Reson. Chem. 38 (2000) 536–542.
[7] L.W. Donaldson, N.R. Skrynnikov, W.-Y. Choy, D.R. Muhandiram, B. Sarkar, J.D. Forman-Kay, L.E. Kay, Structural characterization of proteins with an attached ATCUN motif by paramagnetic relaxation enhancement NMR spectroscopy, J. Am. Chem. Soc. 123 (2001) 9843–9847.
[8] V. Gaponenko, S.P. Sarma, A.S. Altieri, D.A. Horita, J. Li, R.A. Byrd, Improving the accuracy of NMR structures of large proteins using pseudocontact shifts as long/range restraints, J. Biomol. NMR 28 (2004) 205–212.
[9] J. Wöhnert, K.J. Franz, M. Nitz, B. Imperiali, H. Schwalbe, Protein alignment by a coexpressed lanthanide-binding tag for the measurement of residual dipolar couplings, J. Am. Chem. Soc. 125 (2003) 13338–13339.
[10] T. Ikegami, L. Verdier, P. Sakhaii, S. Grimme, P. Pescatore, K. Saxena, K.M. Fiebig, C. Griesinger, Novel techniques for weak alignment of proteins in solution using chemical tags coordinating lanthanide ions, J. Biomol. NMR 29 (2004) 339–349.
[11] G. Pintacuda, A. Moshref, A. Leonchiks, A. Sharipo, G. Otting, Site-specific labelling with a metal chelator for protein-structure refinement, J. Biomol. NMR 29 (2004) 351–361.
[12] J.C. Hus, D. Marion, M. Blackledge, De novo determination of protein structure by NMR using orientational and long-range order restraints, J. Mol. Biol. 298 (2000) 927–936.
[13] I. Bertini, A. Donaire, B. Jiménez, C. Luchinat, G. Parigi, M. Piccioli, L. Poggi, Paramagnetism-based versus classical constraints: An analysis of the solution structure of Ca Ln Calbindin D_{9k}, J. Biomol. NMR 21 (2001) 85–98.
[14] B. Jiménez, L. Poggi, M. Piccioli, Monitoring the early steps of unfolding of di-calcium and mono Ce^{3+} substituted forms of P43M calbindin D_{9k}, Biochemistry 42 (2003) 13066–13073.
[15] F. Kateb, M. Piccioli, New routes to the detection of relaxation allowed coherence transfer in paramagnetic molecules, J. Am. Chem. Soc. 125 (2003) 14978–14979.
[16] G. Pintacuda, M.A. Keniry, T. Huber, A.Y. Park, N.E. Dixon, G. Otting, Fast structure /based assignment of ^{15}N HSQC spectra of selectively ^{15}N labeled paramagnetic proteins, J. Am. Chem. Soc. 126 (2004) 2963–2970.
[17] A. Eletsky, O. Moreira, H. Kovacs, K. Pervushin, A novel strategy for the assignment of side-chain resonances in completely deuterated large proteins using (13) C spectroscopy, J. Biomol. NMR 26 (2003) 167–179.
[18] K. Hu, A. Eletsky, K. Pervushin, Backbone resonance assignment in large protonated proteins using a combination of new 3D TROSY-HN(CA)HA, 4D TROSY-HACANH and 13C detected HACACO experiments, J. Biomol. NMR 26 (2003) 69–77.
[19] I. Bertini, I.C. Felli, R. Kümmerle, D. Moskau, R. Pierattelli, ^{13}C–^{13}C NOESY: An attractive alternative to study large macromolecules, J. Am. Chem. Soc. 126 (2004) 464–465.
[20] I. Bertini, L. Duma, I.C. Felli, M. Fey, C. Luchinat, R. Pierattelli, P. Vasos, A heteronuclear direct detection NMR experiment for protein backbone assignment, Angew. Chem. Int. Ed. 43 (2004) 2257–2259.
[21] I. Bertini, Y.-M. Lee, C. Luchinat, M. Piccioli, L. Poggi, Locating the metal ion in calcium-binding proteins by using cerium(III) as a probe, Chem. Bio Chem. 2 (2001) 550–558.
[22] M. Piccioli, L. Poggi, Tailored HCCH-TOCSY experiment for resonance assignment in the proximity of a paramagnetic center, J. Magn. Reson. 155 (2002) 236–243.
[23] U. Kolczak, J. Salgado, G. Siegal, M. Saraste, G.W. Canters, Paramagnetic NMR studies of blue and purple copper proteins, Biospectroscopy 5 (1999) S19–S32.
[24] T.E. Machonkin, W.M. Westler, J.L. Markley, 13C–13C 2D NMR: A novel strategy for the study of paramagnetic proteins with slow electronic relaxation times, J. Am. Chem. Soc. 124 (2002) 3204–3205.
[25] M. Kostic, S.S. Pochapsky, T.C. Pochapsky, Rapid recycle ^{13}C, ^{15}N and ^{13}C,^{13}C heteronuclear and homonuclear multiple quantum coherence detection for resonance assignments in paramagnetic proteins: Example of Ni^{2+}-containing acireductone dioxygenase, J. Am. Chem. Soc. 124 (2002) 9054–9055.
[26] W. Bermel, I. Bertini, I.C. Felli, R. Kummerle, R. Pierattelli, ^{13}C direct detection experiments on the paramagnetic oxidized monomeric copper, zinc superoxide dismutase, J. Am. Chem. Soc. 125 (2003) 16423–16429.
[27] E. Babini, I. Bertini, F. Capozzi, I.C. Felli, M. Lelli, C. Luchinat, Direct carbon detection in paramagnetic metalloproteins to further exploit pseudocontact shift restraints, J. Am. Chem. Soc. 126 (2004) 10496–10497.
[28] G.A. Caignan, R. Deshmukh, Y. Zeng, A. Wilks, R.A. Bunce, M. Rivera, The hydroxide complex of *Pseudomonas aeruginosa* heme oxygenase as a model of the low/spin Iron(III) hydroperoxide Intermediate in heme catabolism: ^{13}C NMR spectrosocpic studies suggest the active participation of the heme in macrocycle hydroxylation, J. Am. Chem. Soc. 125 (2003) 11842–11852.
[29] T.-M. Chan, J.L. Markley, Nuclear magnetic resonance studies of two-iron-two-sulfur ferredoxins. 5. Hyperfine-shifted peaks in proton and carbon-13 spectra, Biochemistry 22 (1983) 6008.
[30] B.-H. Oh, W.M. Westler, P. Darba, J.L. Markley, Protein carbon-13 spin systems by a single two-dimensional nuclear magnetic resonance experiment, Science 240 (1988) 908–911.
[31] S.S. Sankar, G.N. La Mar, K.M. Smith, E.M. Fujinari, ^{13}C NMR study of labeled vinyl groups in paramagnetic myoglobin derivatives, Biochim. Biophys. Acta 912 (1987) 220–229.
[32] J. Mispelter, M. Momenteau, J.M. Lhoste, Heteronuclear magnetic resonance: Application to biological and related paramagnetic molecules, in: L.J. Berliner, J. Reuben (Eds.), NMR of Paramagnetic Molecules, Plenum Press, New York, 1993.
[33] H. Santos, D.L. Turner, ^{13}C and proton NMR studies of horse ferricytochrome c, FEBS Lett. 194 (1986) 73–77.
[34] Z. Serber, C. Richter, D. Moskau, J.-M. Boehlen, T. Gerfin, D. Marek, M. Haeberli, L. Baselgia, F. Laukien, A.S. Stern, J.C. Hoch, V. Doetsch, New carbon-detected protein NMR experiments using cryoprobes, J. Am. Chem. Soc. 122 (2000) 3554–3555.
[35] B. Vögeli, H. Kovacs, K. Pervushin, Measurements of side chain ^{13}C–^{13}C residual dipolar coupling in uniformly deuterated proteins, J. Am. Chem. Soc. 126 (2004) 2414–2420.
[36] S. Linse, P. Brodin, T. Drakenberg, E. Thulin, P. Sellers, K. Elmden, T. Grundstrom, S. Forsén, Structure–function relationship in EF-hand Ca^{2+}-binding proteins. protein engineering and biophysical studies of calbindin D_{9k}, Biochemistry 26 (1987) 6723–6735.
[37] M. Akke, S. Forsén, W.J. Chazin, Molecular basis for cooperativity in Ca^{2+} binding to calbindin D_{9k}. ^1H nuclear magnetic resonance studies of (Cd^{2+}) 1-bovine calbindin D_{9k}, J. Mol. Biol. 220 (1991) 173–189.
[38] M. Allegrozzi, I. Bertini, M.B.L. Janik, Y.-M. Lee, G. Liu, C. Luchinat, Lanthanide induced pseudocontact shifts for solution structure refinements of macromolecules in shells up to 40 A from the metal ion, J. Am. Chem. Soc. 122 (2000) 4154–4161.
[39] I. Bertini, G. Cavallaro, M. Cosenza, R. Kummerle, C. Luchinat, M. Piccioli, L. Poggi, Cross correlation rates between curie spin and dipole–dipole relaxation in paramagnetic proteins: The case

of cerium substituted calbindin D_{9k}, J. Biomol. NMR 23 (2002) 115–125.
[40] I. Bertini, C.J. Carrano, C. Luchinat, M. Piccioli, L. Poggi, A ^{15}N NMR mobility study on the di-calcium P43M calbindin D_{9K} and its mono La^{3+} substituted form, Biochemistry 41 (2002) 5104–5111.
[41] L.A. Svensson, E. Thulin, S. Forsén, Proline cis-trans isomers in calbindin D_{9k} observed by X-ray crystallography, J. Mol. Biol. 223 (1992) 601–606.
[42] W. Bermel, I. Bertini, L. Duma, L. Emsley, I.C. Felli, R. Pierattelli, P. Vasos, Towards complete assignment of heteronuclear protein resonances by protonless NMR, Angew. Chem. Int. Ed. (2005) in press.
[43] P. Brodin, T. Grundstrom, T. Hofmann, T. Drakenberg, E. Thulin, S. Forsén, Expression of bovine intestinal calcium binding protein from a synthetic gene in *Escherichia coli* and characterization of the product, Biochemistry 25 (1986) 5371–5377.
[44] C. Johansson, P. Brodin, T. Grundstrom, E. Thulin, S. Forsén, T. Drakenberg, Biophysical studies of engineered mutant proteins based on calbindin D9K modified in the pseudo EF-hand, Eur. J. Biochem. 187 (1990) 455–460.
[45] W.J. Chazin, J. Kördel, T. Drakenberg, E. Thulin, P. Brodin, T. Grundstrom, S. Forsén, Proline isomerism leads to multiple folded conformations of calbindin D_{9k}: Direct evidence from two-dimensional 1H NMR spectroscopy, Proc. Natl. Acad. Sci. USA 86 (1989) 2195–2198.
[46] A. Malmendal, G. Carlström, C. Hambraeus, T. Drakenberg, S. Forsén, M. Akke, Sequence and context dependence of EF-hand loop dynamics. An ^{15}N relaxation study of a calcium-binding site mutant of calbindin D_{9k}, Biochemistry 37 (1998) 2586–2595.
[47] L. Emsley, G. Bodenhausen, Optimization of shaped selective pulses for NMR using a quaternion description of their overall propagators, J. Magn. Reson. 97 (1992) 135–148.
[48] D. Marion, K. Wüthrich, Application of phase sensitive correlated spectroscopy (COSY) for measurements of proton-proton spin-spin coupling constants in proteins, Biochem. Biophys. Res. Commun. 113 (1983) 967–974.
[49] A.J. Shaka, P.B. Barker, R. Freeman, Computer-optimized decoupling scheme for wideband applications and low-level operation, J. Magn. Reson. 64 (1985) 547–552.
[50] A.J. Shaka, J. Keeler, R. Freeman, Evaluation of a new broadband decoupling sequence: WALTZ-16, J. Magn. Reson. 53 (1983) 313–340.
[51] I. Bertini, C. Luchinat, R. Macinai, M. Piccioli, A. Scozzafava, M.S. Viezzoli, Paramagnetic metal centers in proteins can be investigated through heterocorrelated NMR spectroscopy, J. Magn. Reson. Ser. B 104 (1994) 95–98.
[52] I. Bertini, C. Luchinat, D. Tarchi, Are true scalar proton-proton connectivities ever measured in COSY spectra of paramagnetic macromolecules?, Chem. Phys. Lett. 203 (1993) 445–449.
[53] P.K. Madhu, P.K. Mandal, N. Muller, Cross-correlation effects involving Curie spin relaxation in methyl groups, J. Magn. Reson. 155 (2002) 29–38.
[54] D.L. Turner, Optimization of COSY and related methods. Applications to ^{1}H NMR of horse ferricytochrome c, J. Magn. Reson. Ser. A 104 (1993) 197–202.
[55] I. Bertini, C. Luchinat, M. Piccioli, D. Tarchi, COSY spectra of paramagnetic macromolecules, observability, scalar effects, cross correlation effects, relaxation allowed coherence transfer, Concepts Magn. Reson. 6 (1994) 307–335.
[56] I. Gelis, N. Katsaros, C. Luchinat, M. Piccioli, L. Poggi, A simple protocol to study blue copper proteins by NMR, Eur. J. Biochem. 270 (2003) 600–609.
[57] L. Müller, Sensitivity enhanced detection of weak nuclei using heteronuclear multiple quantum coherence, J. Am. Chem. Soc. 101 (1979) 4481–4484.
[58] G. Bodenhausen, D.J. Ruben, Natural abundance nitrogen-15 NMR by enhanced heteronuclear spectroscopy, Chem. Phys. Lett. 69 (1980) 185–188.
[59] J.L. Markley, A. Bax, Y. Arata, C.W. Hilbers, R. Kaptein, B.D. Sykes, P.E. Wright, K. Wüthrich, Recommendations for the presentation of NMR structures of proteins and nucleic acids. IUPAC-IUPMB-IUPAB inter-union task group on the standardization of data bases of protein and nucleic acid structures determined by NMR spectroscopy, Eur. J. Biochem. 256 (1998) 1–15.
[60] J.-M. Boehlen, G. Bodenhausen, Experimental aspects of chirp NMR spectroscopy, J. Magn. Reson. Ser. A 102 (1993) 293–301.
[61] M. Zweckstetter, T.A. Holak, An adiabatic multiple spin-echo pulse sequence: removal of systematic errors due to pulse imperfections and off-resonance effects, J. Magn. Reson. 133 (1998) 134–147.
[62] M. Ottiger, F. Delaglio, A. Bax, Measurement of J and dipolar couplings from simplified two-dimensional NMR spectra, J. Magn. Reson. 131 (1998) 373–378.
[63] M.H. Lerche, A. Meissner, F.M. Poulsen, O.W. Sørensen, Pulse sequences for measurement of one-bond (15)N–(1)H coupling constants in the protein backbone, J. Magn. Reson. 140 (1999) 259–263.
[64] I. Bertini, I.C. Felli, R. Kümmerle, C. Luchinat, R. Pierattelli, ^{13}C–^{13}C NOESY: A constructive use of ^{13}C-^{13}C spin-diffusion, J. Biomol. NMR 30 (2004) 245–251.
[65] R. Riek, G. Wider, K. Pervushin, K. Wuthrich, Polarization transfer by cross-correlated relaxation in solution nmr with very large molecules, Proc. Natl. Acad. Sci. USA 96 (1999) 4918–4923.
[66] S. Grzesiek, A. Bax, Improved 3D triple-resonance NMR techniques applied to a 31 kDa protein, J. Magn. Reson. 96 (1992) 432–440.
[67] K. Pervushin, A. Eletsky, A new strategy for backbone resonance assignment in large proteins using a MQ-HACACO experiment, J. Biomol. NMR 25 (2003) 147–152.
[68] N. Shimba, A.S. Stern, C.S. Craik, J.C. Hoch, V. Dötsch, Elimination of $^{13}C_{\alpha}$ splitting in protein NMR spectra by deconvolution with maximum entropy reconstruction, J. Am. Chem. Soc. 125 (2003) 2382–2383.
[69] M. Pellecchia, Y. Pang, L. Wang, A.V. Kurochkin, A. Kumar, E.R.P. Zuiderweg, Quantitative measurement of cross-correlations between ^{15}N and ^{13}CO chemical shift anisotropy relaxation mechanisms by multiple quantum NMR, J. Am. Chem. Soc. 121 (1999) 9165–9170.